Stereochemistry of organic compounds(39) : On the optical contributions and solvent effects of nitrophenyl thioglycopyranosides

その他（別言語等）のタイトル	有機化合物の立体化学(39) : ニトロフェニル L-Pyranosidesの旋光寄与と溶媒効果
著者(英語)	Koko Satsumabayashi, Yoko Nishida, Kiyoshi Tanemura
journal or publication title	Bulletin of the Nippon Dental University. General education
volume	31
page range	77-92
year	2002-03-20
URL	http://doi.org/10.14983/00000554

Stereochemistry of Organic Compounds XXXIX[1)]

On the Optical Contributions and Solvent Effects of Nitrophenyl Thioglycopyranosides

Koko SATSUMABAYASHI, Yoko NISHIDA and Kiyoshi TANEMURA

The Nippon Dental University, School of Dentistry at Niigata,
Hamaura-cho, Niigata 951-8580, JAPAN

(Received November 30, 2001)

In our earlier studies[1-8)], we reported the conformation of various nitrophenyl-glycosides. In the previous paper[1)], the optical contributions of the L-series of pyranosides were investigated using nitrophenyl pentoses and hexoses.

As a result, in the case of the L-series, the signs of the Cotton effects are dominated by the configurations of the chiral centers without any α- and β-types.

Now, this paper deals with D- and L-fucose derivatives (Compounds **I**～**II**) and D-galactose derivatives (Compounds **III**～**IV**) having S atoms at C_1. We also compared Compounds **I**～**IV** with Compounds **V**～**VIII**[1,7)] which do not have S atoms at C_1, namely:

p-Nitrophenyl β-D-1-thiofucopyranoside (Compound **I**),

p-Nitrophenyl β-L-1-thiofucopyranoside (Compound **II**),

o-Nitrophenyl β-D-1-thiogalactopyranoside (Compound **III**),

p-Nitrophenyl β-D-1-thiogalactopyranoside (Compound **IV**),

p-Nitrophenyl β-D-fucopyranoside (Compound **V**)[1)],

p-Nitrophenyl β-L-fucopyranoside (Compound **VI**)[1)],

o-Nitrophenyl β-D-galactopyranoside (Compound **VII**)[7)],

p-Nitrophenyl β-D-galactopyranoside (Compound **VIII**)[7)],

All the compounds that we have examined are illustrated in Figure 1.

For this purpose, the optical contributions were investigated by means of rotatory

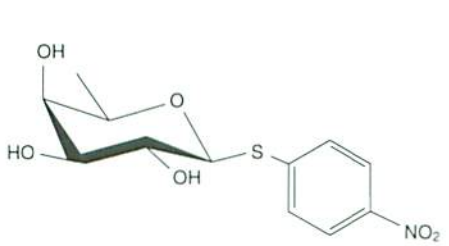

I

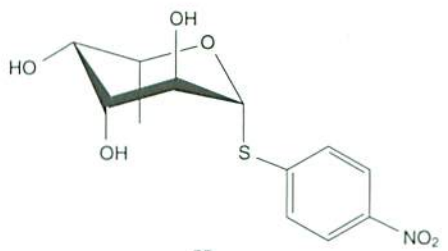

II

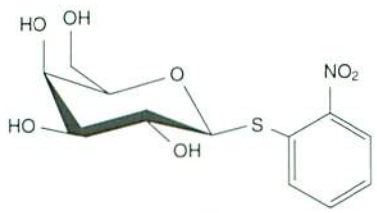

III

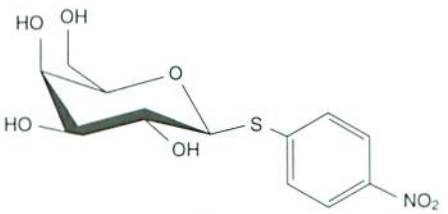

IV

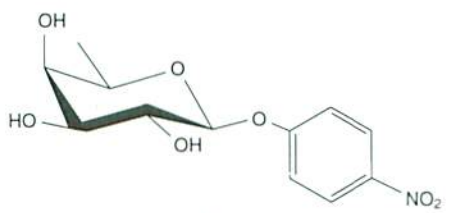

V

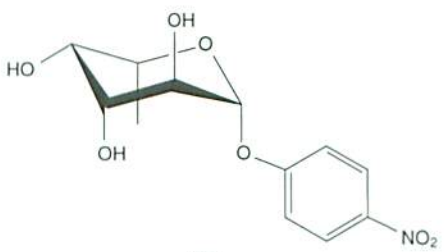

VI

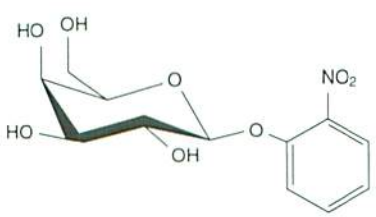

VII

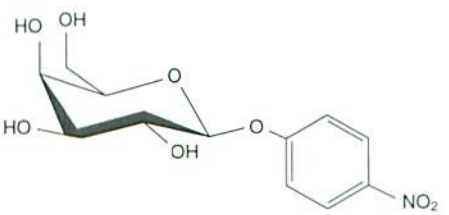

VIII

Figure 1. Compounds I~VIII examined.

dispersion (RD), circular dichroism (CD), and ultraviolet absorption (UV) spectra, using acetonitrile (CH_3CN), ethanol (EtOH) and water (H_2O) as polar solvents and dioxane and tetrahydrofuran (THF) as non-polar solvents. In addition, the proton nuclear magnetic resonance (^{1}H-NMR) spectra were measured in dimethyl sulfoxide-d_6(DMSO-d_6).

Results and Discussion

The RD, CD and UV curves of Compounds **I**~**IV** are shown in Figures 2~5 and

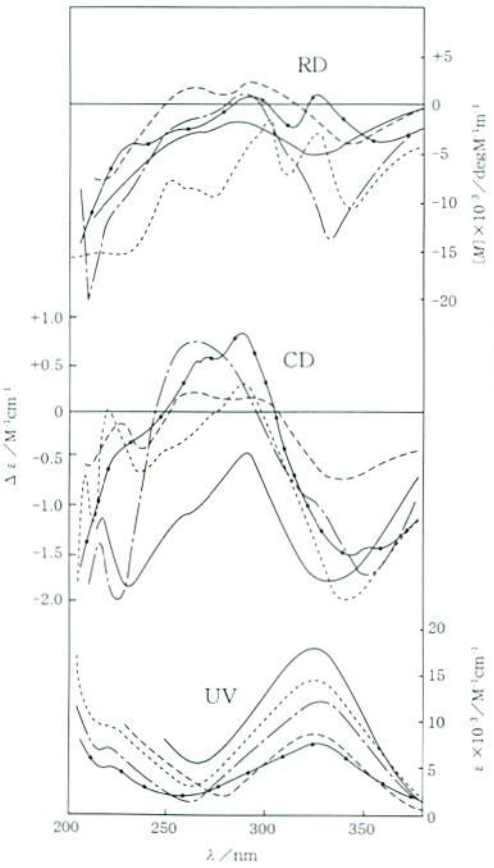

Figure2 RD, CD and UV of **I** (—— in dioxane, – – – – in THF, – – – in CH_3CN, ····· in EtOH, —•—•— in H_2O).

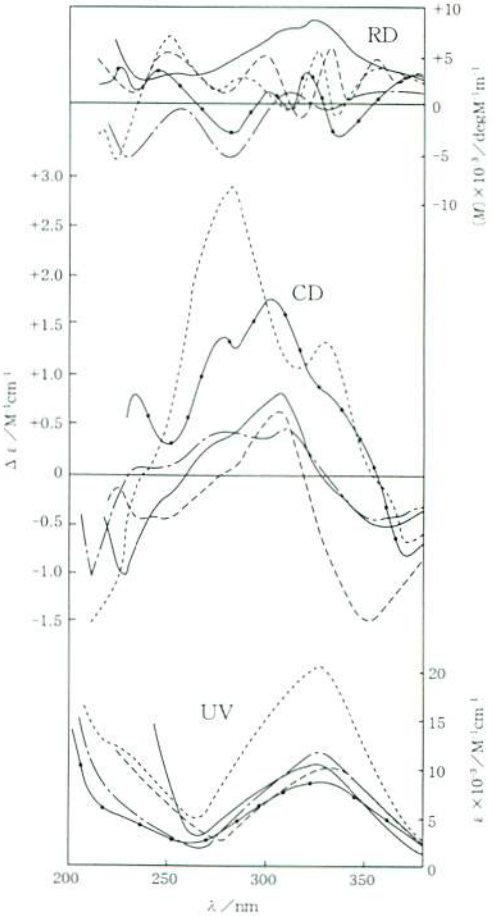

Figure3 RD, CD and UV of **II** (—— in dioxane, – – – – in THF, – – – in CH_3CN, ····· in EtOH, —•—•— in H_2O).

Figures 6～10 in dioxane, tetrahydrofuran, acetonitrile, ethanol and water respectively. The data of RD, CD and UV are summarized in Table 1.

All compounds are β-anomers of pyranosides. Compounds **I**, **III** and **IV** belong to the

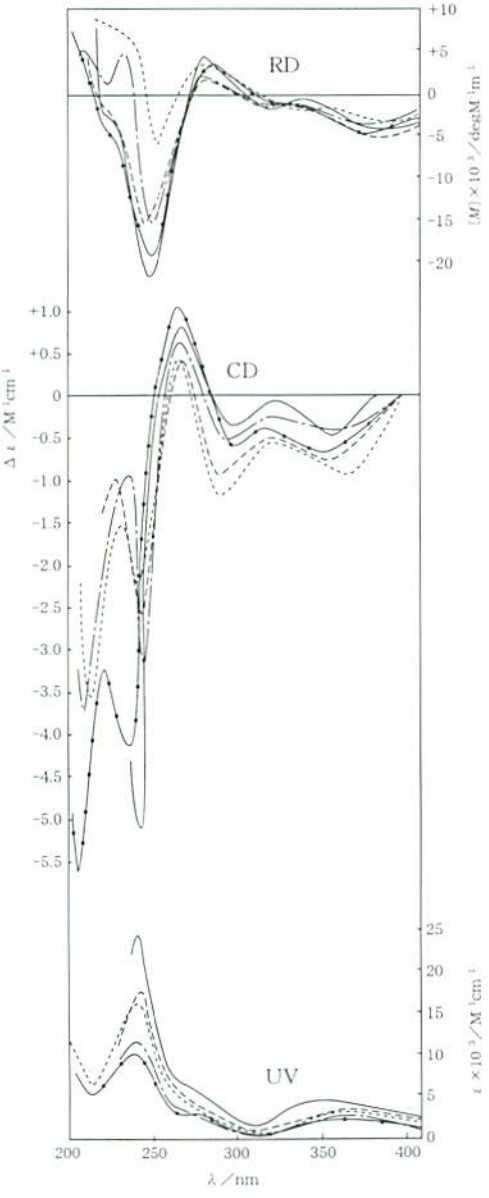

Figure4 RD, CD and UV of **III** (—— in dioxane, – – – – in THF, – – – in CH_3CN, ····· in EtOH, —•—•— in H_2O).

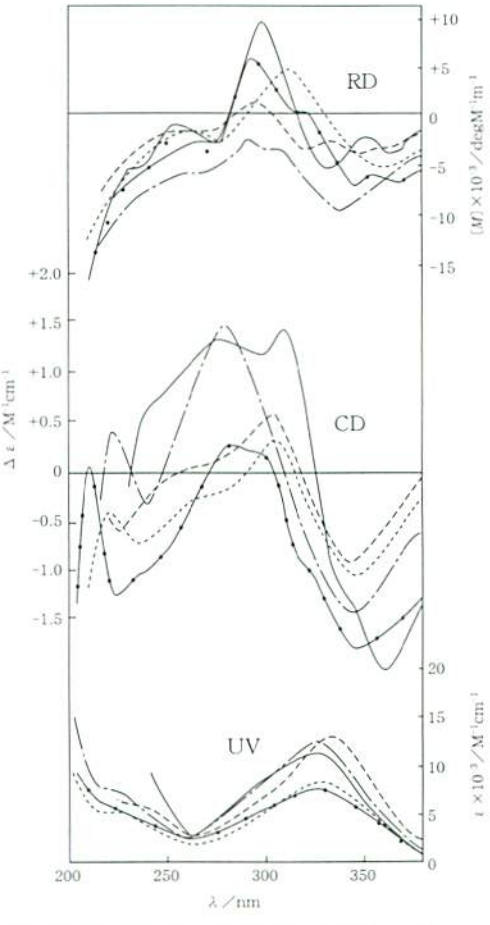

Figure5 RD, CD and UV of **VI** (—— in dioxane, – – – – in THF, – – – in CH_3CN, ····· in EtOH, —•—•— in H_2O).

D-Series, and Compound **II** which is an antipode of Compound **I**, belongs to the L-Series. In **Figures 2~5**, in the case of the D-series, β-anomers (**I**, **III**, **IV**) show negative background rotation, and in the case of the L-series, the β-anomer (**II**) shows positive background rotation, judging from the specific rotation at 589 nm.

As may be seen in **Figures 2~5**, the CD curves of all compounds exhibit the first negative Cotton effects around 336-372 nm due to the $n \rightarrow \pi^*$ transition and complex Cotton effects below 300 nm due to the $\pi \rightarrow \pi^*$ transition in all solvents. In the UV curves of Compounds **I**, **II** and **IV**, the first bands due to the $n \rightarrow \pi^*$ transition appear

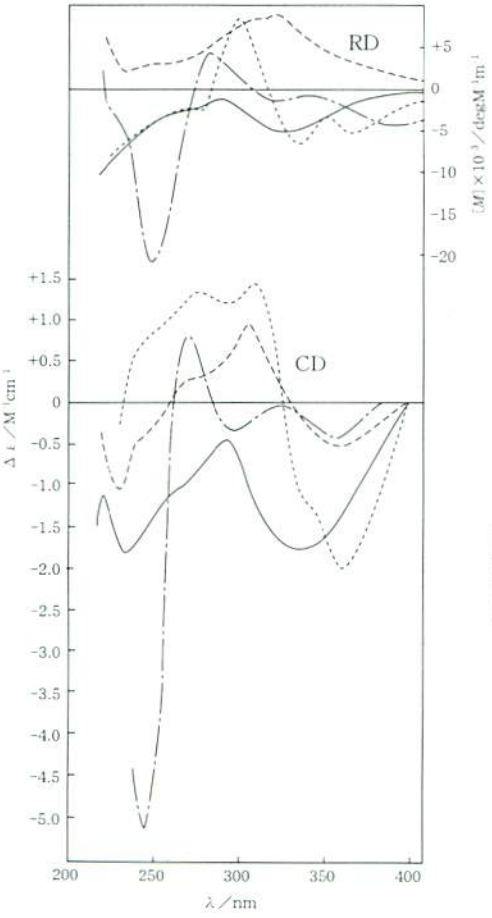

Figure6 RD and CD of **I**, **II**, **III** and **IV** in dioxane (—— **I**, – – – – **II**, – – – **III**, ····· **IV**).

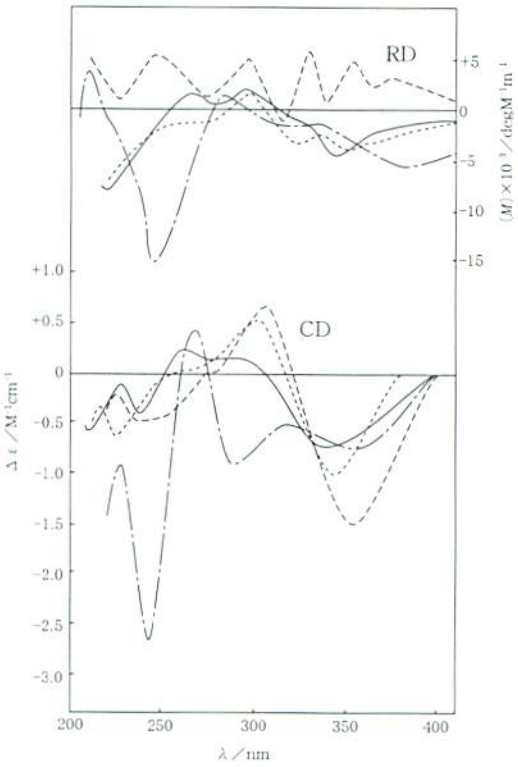

Figure7 RD and CD of **I**, **II**, **III** and **IV** in THF (—— **I**, – – – – **II**, – – – **III**, ····· **IV**).

around 328-335 nm, and the second bands due to the $\pi \rightarrow \pi^*$ transition are suggested below 210 nm with shoulders around 215-245 nm in all solvents. The UV curves of Compound **III** show the first bands due to the $n \rightarrow \pi^*$ transition appear around 328-335 nm, and the second bands due to the $\pi \rightarrow \pi^*$ transition around 240-244 nm in all solvents clearly. That is, in the case of Compound **III**, the effect of the *ortho*-nitro group does not cause any vibrations in the charge-transfer absorption bands and those bands shift to the longer wavelength region.

To begin with, let's examine the optical contributions of Compound **I** and its antipode, **II**. Figures 11 and 12 are comparisons between Compounds **I** and **II** together with comparisons between Compounds **V**[1] and **VI**[1]. For reference, the measurement results of Compounds **V** and **VI** in THF solvent which were not in a previous paper, have been added to Figures 11 and 12. When the first Cotton effects

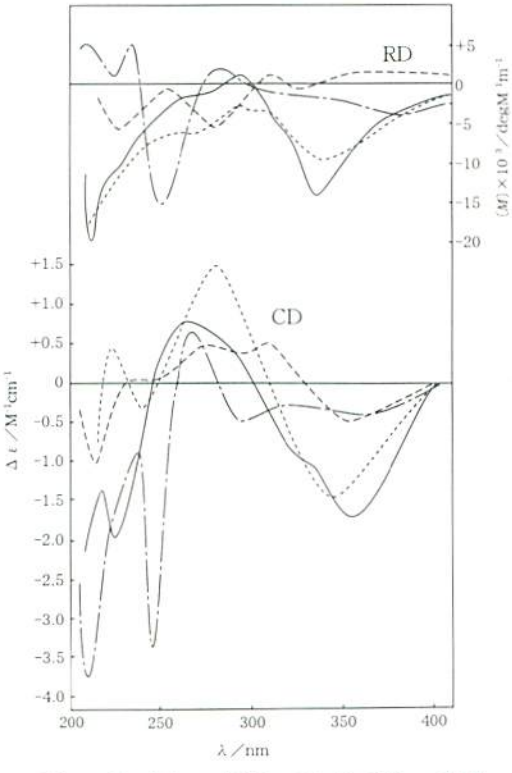

Figure8 RD and CD of **I**, **II**, **III** and **IV** in CH_3CN (—— **I**, – – – – **II**, – – – **III**, ····· **IV**).

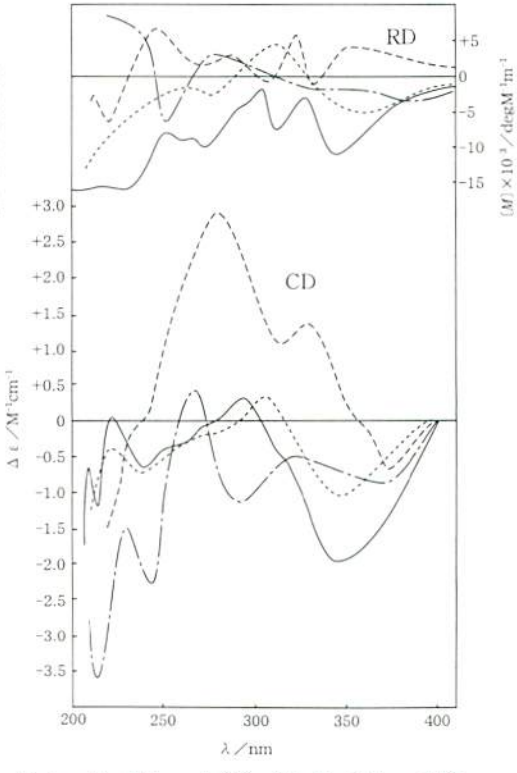

Figure9 RD and CD of **I**, **II**, **III** and **IV** in EtOH (—— **I**, – – – – **II**, – – – **III**, ····· **IV**).

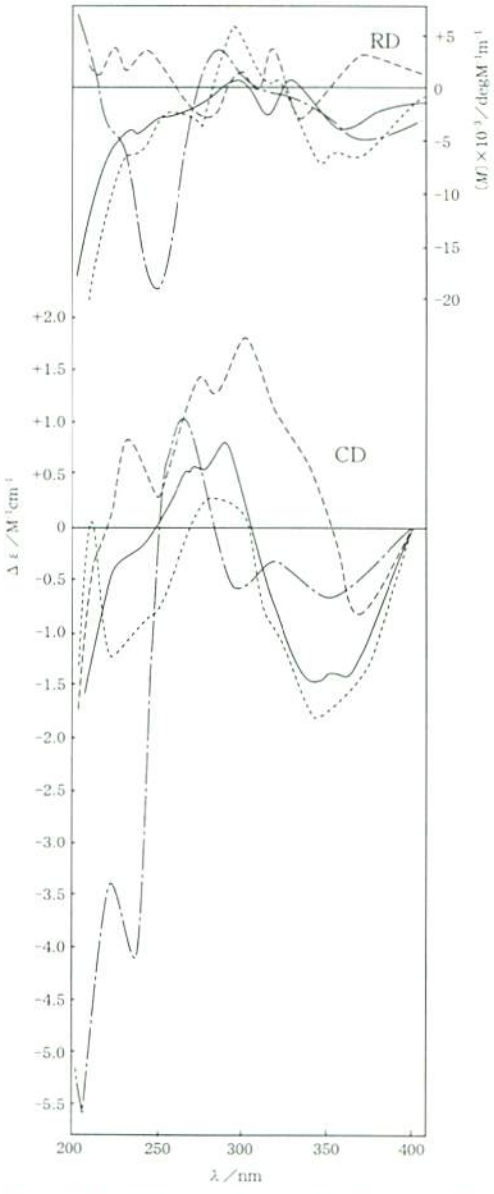

Figure 10 RD and CD of **I**, **II**, **III** and **IV** in H_2O (—— **I**, – – – – **II**, – – – **III**, ····· **IV**).

Table 1 Data of CD, RD and UV spectra

Compound	spectrum	solvent	λ_{max}/nm($\Delta\varepsilon$/$M^{-1}cm^{-1}$;[M]/deg $M^{-1}m^{-1}$;ε/$M^{-1}cm^{-1}$)
I	CD	dioxane	336(−1.79), 234(−1.85)
		THF	339(−0.719), 288(+0.170), 266(+0.203), 239(−0.401), 212(−0.592)
		CH_3CN	355(−1.71), 264(+0.783), 226(−1.91)
		EtOH	342(−1.99), 293(+0.316), 239(−0.670), 221(+0.0200) 213(−1.23)
		H_2O	365(−1.44), 346(−1.49), 290(+0.820), 270(+0.564) 267(+0.543)
	RD	dioxane	434(−668, I*), 330(−5240), 328(−5230), 326(−5240), 288(−1720), 256(−3520, I)
		THF	484(−425, I), 342(−4610), 329(−1610, I), 296(+2020), 282(+327), 265(+1060), 221(−8340)
		CH_3CN	522(−470, I), 335(−14500), 322(−8280, I), 294(+1040), 270(−1630), 264(−1590), 220(−12100, I), 211(−20500)
		EtOH	512(−672, I), 346(−11000), 329(−2850), 214(−7740), 304(−1540), 294(−4280, I), 275(−9730), 266(−8930), 260(−8950), 254(−7960), 232(−15700), 221(−15400), 203(−15800)
		H_2O	522(−607, I), 363(−3850), 327(+980), 316(−2830), 295(+569), 253(−2780, I), 238(−4250), 231(−4120)
	UV	dioxane	329(17500)
		THF	335(8430)
		CH_3CN	331(11700), 221(6210)
		EtOH	329(14000), 246−216(5880−9030, shoulder)
		H_2O	329(7690), 221(4740)
II	CD	dioxane	362(−0.527), 306(+0.862), 231(−1.08)
		THF	354(−1.48), 306(+0.651), 239(−0.469)
		CH_3CN	351(−0.473), 309(+0.520), 275(+0.482), 233(+0.0433), 214(−1.08)
		EtOH	372(−0.712), 329(+1.38), 281(+2.92)
		H_2O	370(−0.848), 301(+1.83), 275(+1.44), 233(+0.850)
	RD	dioxane	322(+8730), 315(+8150), 309(+8180), 254(+2630, I), 234(+1930)
		THF	534(+484, I), 428(+776, I), 375(+3290), 364(+2520), 353(+4740), 340(+601), 330(+6020), 316(−1040), 297(+5130), 275(+2050), 247(+5310), 228(+654)
		CH_3CN	362(+1790), 327(−603), 308(+1330), 279(−5640), 253(−247), 228(−5920)
		EtOH	512(+713, I), 354(+4120), 333(−1340), 324(+5720), 310(−650), 287(+2940), 273(+1390), 248(+6900), 223(−6230), 214(−2480)
		H_2O	373(+3150), 334(−3200), 318(+3430), 308(−560), 300(+1760), 279(−3130), 242(+3490), 230(+1050), 214(+3890), 216(+1110)
	UV	dioxane	331(10300)
		THF	333(9910)

		CH_3CN	330(11500), 239−215(4630−8310, shoulder)
		EtOH	329(20000), 242−216(8690−12400, shoulder)
		H_2O	330(8470), 242−215(3290−6250, shoulder)
III	CD	dioxane	358(−0.453), 296(−0.358), 269(+0.835), 244(−5.13)
		THF	353(−0.750), 290(−0.939), 267(+0.446), 243(−2.71)
		CH_3CN	356(−0.392), 293(−0.510), 267(+0.671), 245(−3.52), 210(−3.77)
		EtOH	369(−0.898), 292(−1.19), 267(+0.422), 244(−2.28), 214(−3.67)
		H_2O	354(−0.697), 298(−0.612), 266(+1.06), 237(−4.16), 206(−5.61)
	RD	dioxane	516(−1230, I), 388(−4360), 340(−818), 319(−1720), 282(+4050), 249(−21700), 230(−3720, I)
		THF	386(−5580), 332(−1370), 316(−1550), 282(+1710), 245(−15400), 226(−2700, I), 211(+4010)
		CH_3CN	382(−3670), 336(−1760, I), 279(+2010), 251(−15400), 233(+4860), 225(−910), 209(+4980)
		EtOH	512(−1180, I), 394(−3370), 354(−1950, I), 281(+3430), 254(−6120)
		H_2O	374(−4830), 328(−1080, I), 285(+3480), 250(−19200), 230(−5210, I)
	UV	dioxane	362(4430), 292−264(2760−6960, shoulder), 243(24500)
		THF	367(3440), 294−266(2090−5600, shoulder), 244(17500)
		CH_3CN	360(2480), 290−272(1920−3240, shoulder), 242(11900)
		EtOH	361(3350), 292−268(2030−4910, shoulder), 243(16300)
		H_2O	363(2340), 278(3190), 240(10600)
IV	CD	dioxane	361(−2.01), 309(+1.46), 277(+1.36)
		THF	345(−0.991), 303(+0.571), 226(−0.626)
		CH_3CN	345(−1.46), 281(+1.50), 241(−0.348), 223(+0.452)
		EtOH	346(−1.08), 315(+0.333), 237(−0.724)
		H_2O	346(−1.80), 282(+0.281), 225(−1.27), 212(+0.0578)
	RD	dioxane	512(−566, I), 365(−5400), 352(−3570), 334(−6860), 300(+8180), 278(−2680), 269(−2580)
		THF	565(−372, I), 464(−586, I), 365(−3070, I), 348(−3850), 335(−2330), 321(−3030), 296(+1480), 275(−1310), 264(−1280)
		CH_3CN	340(−9440), 304(−3230), 303(−3250), 290(−2560), 269(−6100), 262(−5840)
		EtOH	363(−5340), 314(+4400), 279(−2710), 265(−1670)
		H_2O	512(−593, I), 369(−6750), 355(−6070), 347(−7050), 325(+525), 317(+101), 295(+5640), 277(−4020), 254(−2330), 239(−6590), 232(−6530)
	UV	dioxane	328(11100)
		THF	335(12800), 256−231(3400−5950, shoulder)
		CH_3CN	329(12000), 244−215(4300−7720, shoulder)
		EtOH	329(8310), 246−215(3300−5190, shoulder)
		H_2O	328(7580), 236−216(4000−6090, shoulder)

*[1]Inflection point

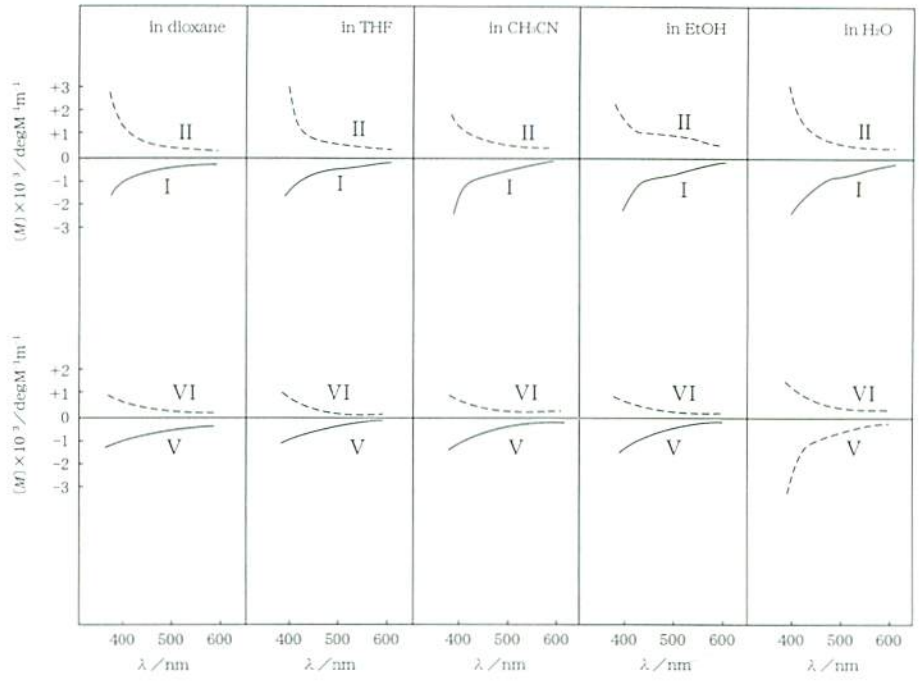

Figure 11 RD of two sets of antipodes, I — II and V — VI.

in the CD curves of Compound II are compared with Compound I, the maximum values are small and these bands shift to the long-wavelength side except in the THF solvent, a result identical to the oxygen counterparts, V and VI. In the meantime, the second Cotton effects of Compound II show clarified and positive peaks at 301-329 nm. The RD curves of the long-wavelength side (380-600 nm) show the clear enantiomeric symmetry in Figure 11. Since the wavelengths separate from the absorption bands, there are small effects of the absorption bands, and as a result, the effects of the background appear strongly. The configuration of each asymmetric carbon and the values of specific rotation at 589 nm of Compounds I, II, V and VI are shown in Tables 2 and 3. As it was described above, the CD curves show no symmetry in all solvents, the first Cotton effects of Compounds I, II and V are negative in all solvents as may be seen in Figure 12. In the case of Compound VI, the first Cotton effects are negative in non-polar solvents, and positive in polar solvents around 310-340 nm as seen in Figure 12. It is evident that the oxygen Compound VI is affected by polar solvents, CH_3CN, EtOH and H_2O. It is considered that the polar solvents could form the

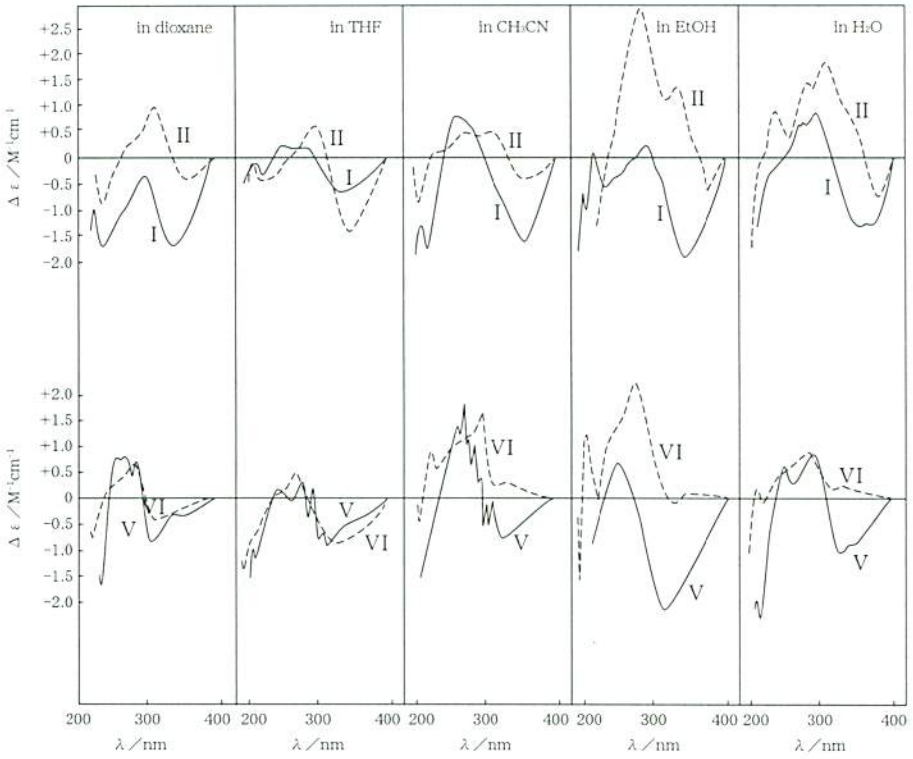

Figure 12 CD of two sets of antipodes, **I**—**II** and **V**—**VI**.

Table 2 Configurations of Asymmetric Carbons

Compound	Type of Anomer	C_1	C_2	C_3	C_4	C_5
I, **V**	D-β	S	R	S	S	R
II, **VI**	L-β	R	S	R	R	S

Table 3 $[\alpha]_{589}$ (deg, $l=1$ cm, c≒1 g/ml^{-1}) in all Solvents at 25°C

Compound	dioxane	THF	CH_3CN	EtOH	H_2O
I	−341	−210	−218	−350	−341
II	+241	+431	+363	+421	+387
V	−269	−108	−72.3	−111	−272
VI	+301	+63.1	+229	+198	+286

intermolecular bonds between themselves and the compound, therefore, the stable conformation changes in polar solvents.

The axiom "The antipode contributes to the opposite optical rotation" can be applied to the long wavelength region, the D-line, but cannot be applied to the signs of the Cotton effects. The reason is the preferable conformer changes into stablized axial hydroxyl groups and an *ortho*-nitrophenyl group of sugar.

Judging from **Figure 11** and **Table 3**, the sulfur compounds contribute large rotations in RD showing good enantiomeric symmetry and small solvent dependency in comparison with the oxygen compounds. It is proven that the *p*-nitrophenyl group, which received the solvent effect, affects the optical rotatory contribution of C_1^*, because the covalent bond radius of O (0.74 Å) is shorter than the covalent bond radius of S (1.04 Å).

It is possible to estimate the optical contribution of C_5 from the RD and CD curves, since the structures of Compounds **I** and **IV** differ only at the C_5 substituent. When the RD curves of Compound **I** were compared with the RD curves of **IV**, both specific rotations have the negative maximum in the 330-600 nm wavelength region in all solvents. When the CD curves were compared, though the first Cotton effects take various values within the 336-365 nm wavelength and $\Delta\varepsilon$ -0.719～-1.99, the superior difference is not recognized, as shown by **Figure 13**. Therefore, there is no need to consider the difference between the optical contribution of C_5-CH_3 and C_5-CH_2OH.

In **Figure 14**, the CD curves of Compounds **I** to **VIII** are mapped. Compounds **I** to **IV** have a sulfur atom at C_1 while Compounds **V** to **VIII** have an oxygen atom at C_1.

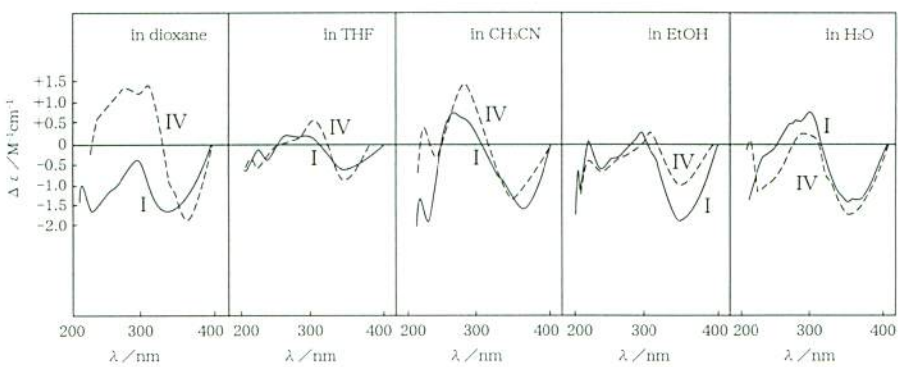

Figure 13 CD of **I** and **IV**.

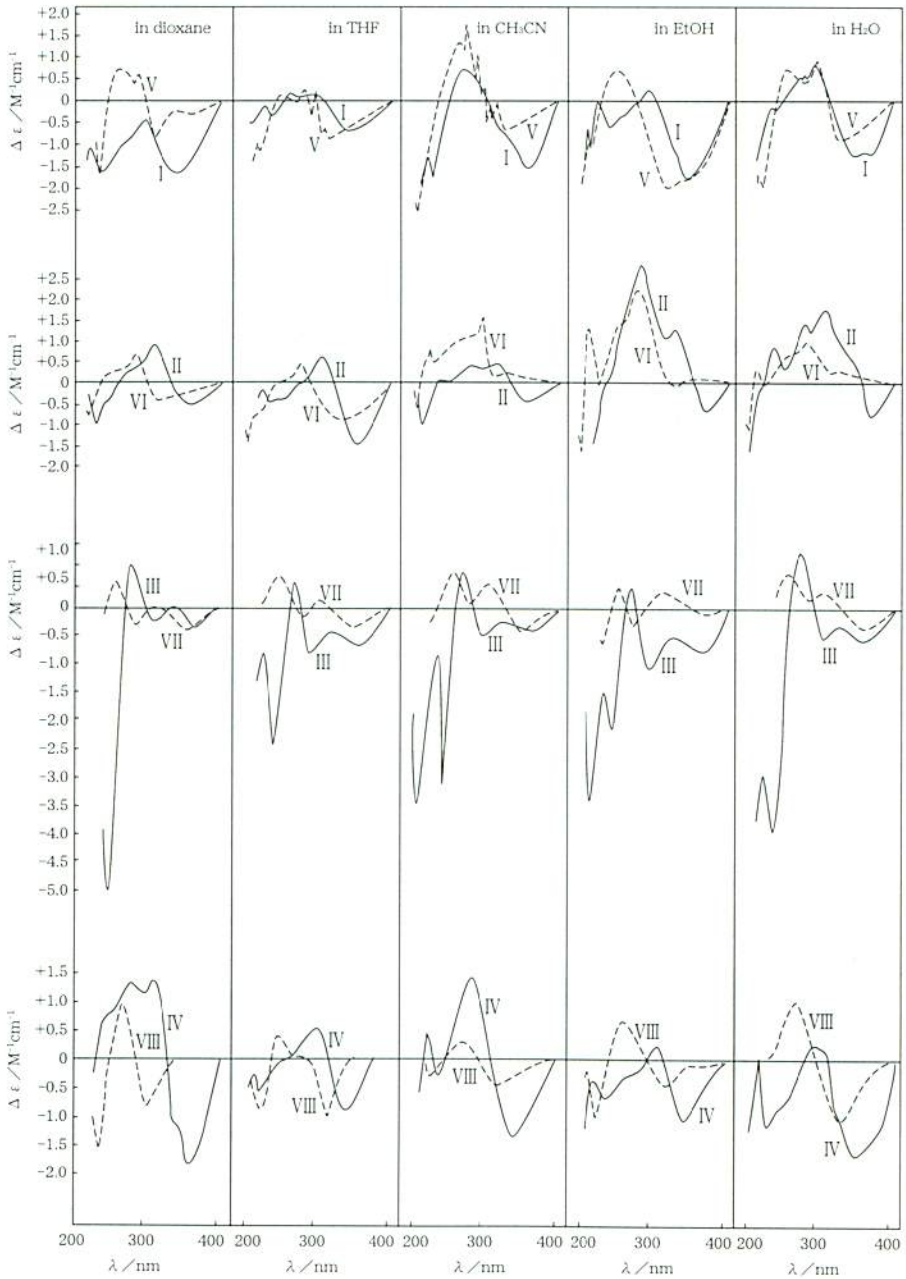

Figure14 CD of thioglycosides (**I, II, III, IV**) and glycosides (**V, VI, VII, VIII**).

Compound **I** is compared with Compound **V**, Compound **II** with Compound **VI**, Compound **III**, with Compound **VII**, and Compound **IV**, with Compound **VIII**. The position of the first Cotton effects of the sulfur compounds (**V**～**IV**) shift to the long wavelength in comparison with the oxygen compounds (**V**～**VIII**). However, though the distance between S and C_1^* is greater than the distance between O and C_1^*, optical rotatory contributions due to the *p*-nitrophenyl group vary irregularly in non-polar and

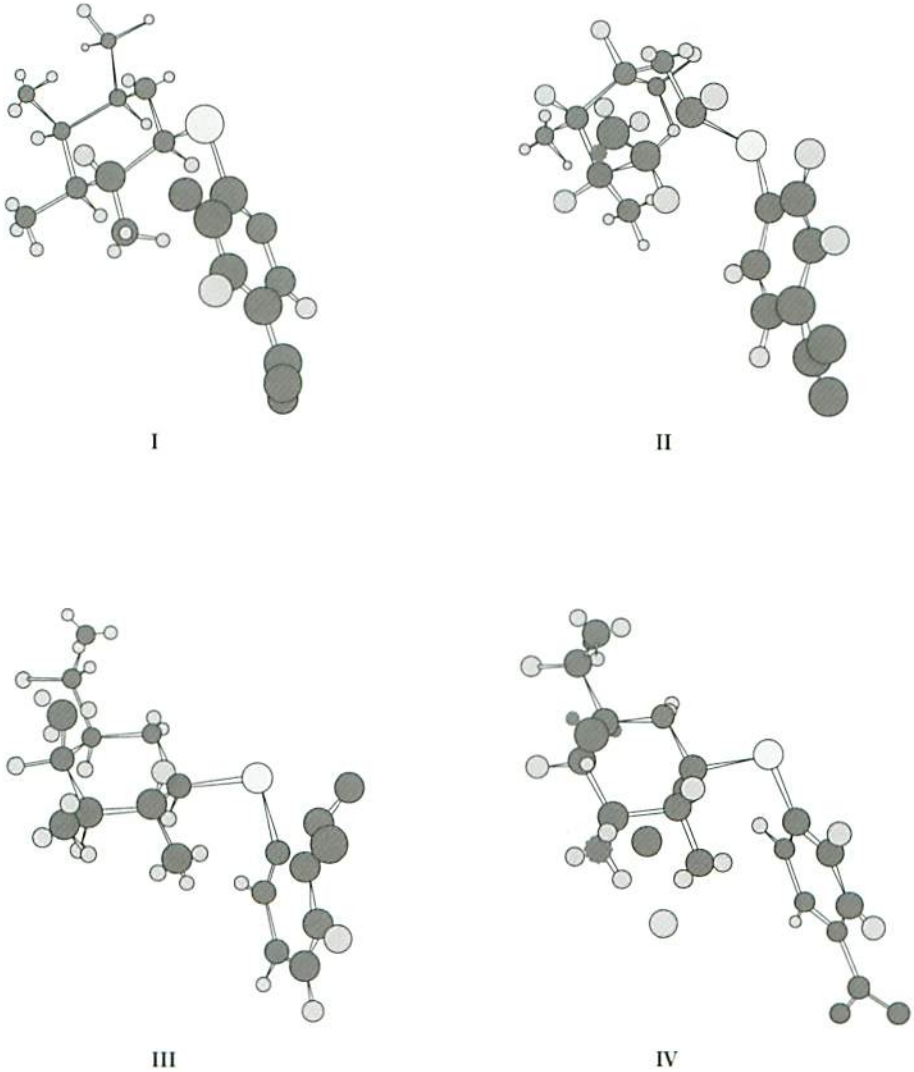

Figure15 Energy minimized molecular model of **I** ～ **IV**.

polar solvents. In the meantime, in the case of **III** and **VII**, which substitutes the sulfur atom of **III** at C_1 with an oxygen atom, the RD and CD curves are hardly affected by the difference between the solvents. This indicates that Compounds **III** and **VII** have rigid structures because the formation of sugar residue is fixed by the *o*-nitrophenyl group. In the case of Compound **III**, the complex Cotton effects due to the transition of the phenyl group exhibit clearly positive signs at 266-269 nm and negative signs at 237-245 nm respectively.

In order to investigate the conformation of Compounds **I**~**IV**, geometry optimizations were carried out using MM2 calculations. **Figure 15** shows the molecular structures created by the calculations using minimized energy. It is possible that all structures in **Figure 15** propose the preferable conformation.

To summarize, the structures of the sulfur compounds are more stable in comparison with the oxygen compounds. The following conclusions could be reached:

1. The background rotations in RD of thioglycosides are larger and solvent dependencies are smaller than their oxygen counterparts.
2. Because of the rigid structures of the *o*-nitrophenyl derivatives, the solvent dependencies are small in comparison with the *p*-nitrophenyl derivatives.
3. The axiom "The antipode contributes to the opposite optical rotation" can be applied to the long wavelength region (in **Figure 11**).
4. The information from the CD characteristics is useful for the speculation of the conformation.

Experimental

Measurements. The RD and CD were measured in dioxane, tetrahydrofuran, acetonitrile, ethanol and water at 25°C, in the wavelength region from 200 to 600 nm with a JASCO/UV-5 type optical rotatory dispersion recorder. The UV spectra were measured under the same conditions as the RD and CD measurements by a SHIMADZU UV-2550 PC Spectrophotometer. The ^{1}H-NMR spectra were measured on a Hitachi Model R-24B at room temperature in DMSO-d_6 as a solvent. Chemical shifts are in ppm (δ) from $SiMe_4$ as the internal standard and J-values are given in Hz.

Materials. All the compounds were obtained from commercial suppliers and were

used without further purification.

p-Nitrophenyl β-D-1-thiofucopyranoside (Compound **I**). mp 164°C; ^{1}H-NMR δ=1.17 (d, J=6.2 Hz, 3H), 3.18-4.02 (m, 4H), 4.61 (d, J=4.6Hz, 1H), 4.76-5.04 (m, 2H), 5.30 (d, J=5.2Hz, 1H), 7.64 (d, J=9.2 Hz, 2H) and 8.18 (d, J=9.2 Hz, 2H).

p-Nitrophenyl β-L-1-thiofucopyranoside (Compound **II**). mp 175°C; ^{1}H-NMR δ=1.16 (d, J=6.4 Hz, 3H), 3.19-4.01 (m, 4H), 4.57 (d, J=4.8 Hz, 1H), 4.73-5.02 (m, 2H), 5.26 (d, J=5.2 Hz, 1H), 7.60 (d, J=9.2 Hz, 2H) and 8.14 (d, J=9.2 Hz, 2H).

o-Nitrophenyl β-D-1-thiogalactopyranoside (Compound **III**). mp 196°C; ^{1}H-NMR δ= 3.19-3.96 (m, 6H), 4.44-5.04 (m, 4H), 5.33 (d, J=5.6 Hz, 1H) and 7.23-8.29 (m, 4H).

p-Nitrophenyl β-D-1-thiogalactopyranoside (Compound **IV**). mp 167°C; ^{1}H-NMR δ= 3.16-3.94 (m, 6H), 4.38-5.10 (m, 4H), 5.28 (br s, 1H), 7.64 (d, J=9.2 Hz, 2H) and 8.13 (d, J=8.8 Hz, 2H).

References

1) K. Satsumabayashi, Y. Nishida and K. Tanemura, This Bulletin, **30**, 75 (2001).
2) K. Satsumabayashi, Y. Nishida and K. Tanemura, *ibid*., **29**, 71 (2000).
3) K. Satsumabayashi, Y. Nishida and K. Tanemura, *ibid*., **28**, 51 (1999).
4) K. Satsumabayashi, Y. Nishida and K. Tanemura, *ibid*., **27**, 55 (1998).
5) K. Satsumabayashi, Y. Nishida and K. Tanemura, *ibid*., **25**, 43 (1996).
6) K. Satsumabayashi, Y. Nishida and K. Tanemura, *ibid*., **24**, 95 (1995).
7) K. Satsumabayashi, Y. Nishida and K. Tanemura, *ibid*., **23**, 59 (1994).
8) K. Satsumabayashi, and Y. Nishida, *ibid*., **16**, 89 (1987).